

Macro- vs Microphase Separation in Copolymer/Homopolymer Mixtures

Tao Pan, Kanglin Huang, and Anna C. Balazs*

Materials Science and Engineering Department, University of Pittsburgh, Pittsburgh, Pennsylvania 15261

Martin S. Kunz,[†] Anne M. Mayes,[‡] and Thomas P. Russell*

IBM Research Division, Almaden Research Center, 650 Harry Road, San Jose, California 95120-6099

Received October 14, 1992; Revised Manuscript Received March 1, 1993

ABSTRACT: Monte Carlo simulations were used to model mixtures of symmetric diblock copolymers and a fixed volume fraction (10%) of homopolymer. However, the homopolymer molecular weights were varied from 2, 5, and 10 times that of the corresponding block in the copolymer. It is found that, when the homopolymer molecular weight becomes significantly greater than that of the corresponding copolymer block, the homopolymer forms aggregates. These aggregates are highly localized in space and form bridges between adjacent lamellar microdomains. The presence of these aggregates does not, however, perturb the underlying lamellar morphology. These results are shown to be in qualitative agreement with transmission electron microscopy studies on thin films of homopolymer/diblock copolymer mixtures of similar, relative molecular weights.

Introduction

Investigations into the phase behavior of block copolymers continue to reveal new and complex morphologies for the microphase-separated melts. In particular, the chains can form ordered arrays of spheres, cylinders, or lamellae or continuous networks, such as double-diamond^{1,2} or interconnected lamellar^{3,4} structures. Since the morphology greatly influences the behavior of these materials, block copolymers can be tailored to display a range of rheological, mechanical, and optical properties. The morphology of the system can be further controlled by blending block copolymers with homopolymer chains. Recent experimental⁵⁻¹⁰ and theoretical^{10,11} studies have revealed the conformation of A homopolymers in the lamellar phase of AB diblocks. The results show that the homopolymers are confined to the A domains and can swell the copolymer chains laterally. In these studies, however, the length of the homopolymer was less than or comparable to the length of the A block in the copolymer. In modeling these systems,^{10,11} only a single lamellar microdomain was considered. Furthermore, the self-consistent field calculations were solved only in one dimension, yielding polymer density profiles perpendicular to the lamellar axis. While these approximations are necessary in such analytical descriptions, significant structural details can be lost.

In this paper, a Monte Carlo computer simulation is used to examine the phase behavior of mixtures of AB symmetric, diblock copolymers with A homopolymers. We focus our attention on cases where the homopolymer concentration is relatively low (10%), but the chains are significantly longer than the A block in the copolymer. These results are then compared to experimental studies on mixtures of polystyrene, PS, with symmetric, diblock copolymers of PS and poly(methyl methacrylate), PMMA, denoted P(S-*b*-MMA).

Computer simulations provide a significant advantage in these studies since no a priori assumptions are made

about the geometry of the system. Rather, the molecules are allowed to self-assemble into the preferred microstructure.¹² Thus, the model can provide significant geometric information about the three-dimensional conformation of the homopolymers, as well as the morphology of the diblock copolymer microdomains. Furthermore, the graphical output from the simulations allows a visualization of these complex structures. The computer-generated images also facilitate direct comparison between simulation results and experimental micrographs. As will be shown below, both methods yield similar images of an unusual microphase morphology in homopolymer/diblock blends.

Simulations

Larson^{12,13} developed Monte Carlo (MC) simulations to model the behavior of amphiphilic chains in oil/water mixtures. The methodology is equally applicable to AB diblocks in a solvent composed of A and B monomers. We extended the model by introducing the A homopolymers. Since the simulations are identical in all other respects, only a brief summary of the technique is provided. In the model, the molecules are confined to a cubic lattice. The cube in our simulations is 20 lattice sites on each side. Periodic boundary conditions are imposed on all sides of this box. The homopolymer and diblock copolymer chains occupy a sequence of adjacent or diagonally adjacent sites. The length of the diblock is fixed at 8 sites, with four A and four B sites. Homopolymer lengths of 8, 20, and 40 A sites were considered. The volume fractions of diblock and homopolymer are fixed at 85% and 10%, respectively. (Thus, as the length of the homopolymer is increased, fewer of these chains are placed in the box in order to maintain the specified volume percent. Specifically, there are 20 homopolymers of length 40, 40 of length 20, and 100 homopolymers of length 8.) A small volume fraction (5%) of solvent or A monomers, which occupy single sites, was included in the modeling. Since there are no void sites in this simulation (as sites are occupied by either solvent or chain sites), these single sites are necessary for the chains to undergo structural rearrangements.

Three types of molecular movements are allowed in the simulation: the positions of two solvent sites can be

* Present address: CIBA GEIGY Ltd., Basel, Switzerland.

[†] Present address: MIT, Department of Materials Science, Cambridge, MA 02139.

Table I^a

ω	no. of steps ($20 \times 20 \times 20$ lattice)
0.0308	30 000 000
0.0615	75 000 000
0.0923	75 000 000
0.1231	150 000 000
0.1385	300 000 000
0.1538	300 000 000

^a Starting from $T = \infty$ ($\omega = 0$), ω is systematically increased (system is "cooled") as shown.

interchanged, while the chains can undergo kink and reptative moves. The Metropolis algorithm is implemented to determine if a specific move is to be executed. In particular, if a move causes the same type of sites to exchange positions (an A interchanges with an A or B with B), the move is accepted with unit probability. If, however, the move results in an A site changing positions with a B site (or vice versa), the move is accepted with a probability of $e^{-\omega}$, where $\omega = (W/k_B T)$ is the only energetic parameter in the system. W is the net energy of mixing, k_B is Boltzmann's constant, and T is the absolute temperature. Thus, ω corresponds to an inverse dimensionless temperature and is equivalent to the Flory-Huggins χ parameter.

At the start of the simulation, ω is set equal to zero (corresponding to infinite temperature) and the molecules are randomly dispersed on the lattice. The system is then slowly cooled by increasing ω incrementally, with a sufficiently large number of MC steps between each increment so that the system can achieve thermal equilibrium at each stage of the simulation. (The detailed cooling scheme is listed in Table I.)

As the temperature is lowered, the probability of interchanges between the A and B units decreases and, consequently, the mixtures will phase separate. At the final value of $\omega = 0.1538$,¹⁴ Larson observed lamellae and ordered arrays of cylinders and spheres that characterize the morphologies of microphase-separated diblocks.¹³ Thus, the prescribed cooling scheme will also locate our results in the microphase-separated regime.¹⁵

Upon completion of the simulation, the cubic lattice is subdivided into layers parallel to a face of the cube and the microphase-separated morphology in each layer can be examined. Parts a and b of Figure 1 show two slices for the case where the homopolymer is 8 lattice sites long (twice the A block length). The actual slice has dimensions of 20×20 units. The 80×80 figure is filled by periodic images. The symbol \blacksquare represents the A sites, and the blank region denotes the B sites of the diblock copolymer. Dark dots are the location of the A homopolymer, and the small number of A solvent sites are represented by the empty squares. The figures clearly show a lamellar morphology. As expected, small concentration variations of each component are seen in going from slice to slice; but overall, the homopolymer is uniformly dispersed from slice to slice and is incorporated within the A lamellar microdomains.

To further characterize the system, we focused on one A microdomain. (Recall that one microdomain is composed of two opposing A "brushes".) Using a least squares fit, the plane that cuts through the middle of the A layer is determined, and the homopolymer density profile normal to this plane is obtained. As shown in Figure 2, the short homopolymer is localized in the center of the layer, i.e., between the two A brushes. This observation agrees qualitatively with the conclusions obtained from self-consistent field calculations^{10,11} and with recent neutron reflectivity measurements.⁹

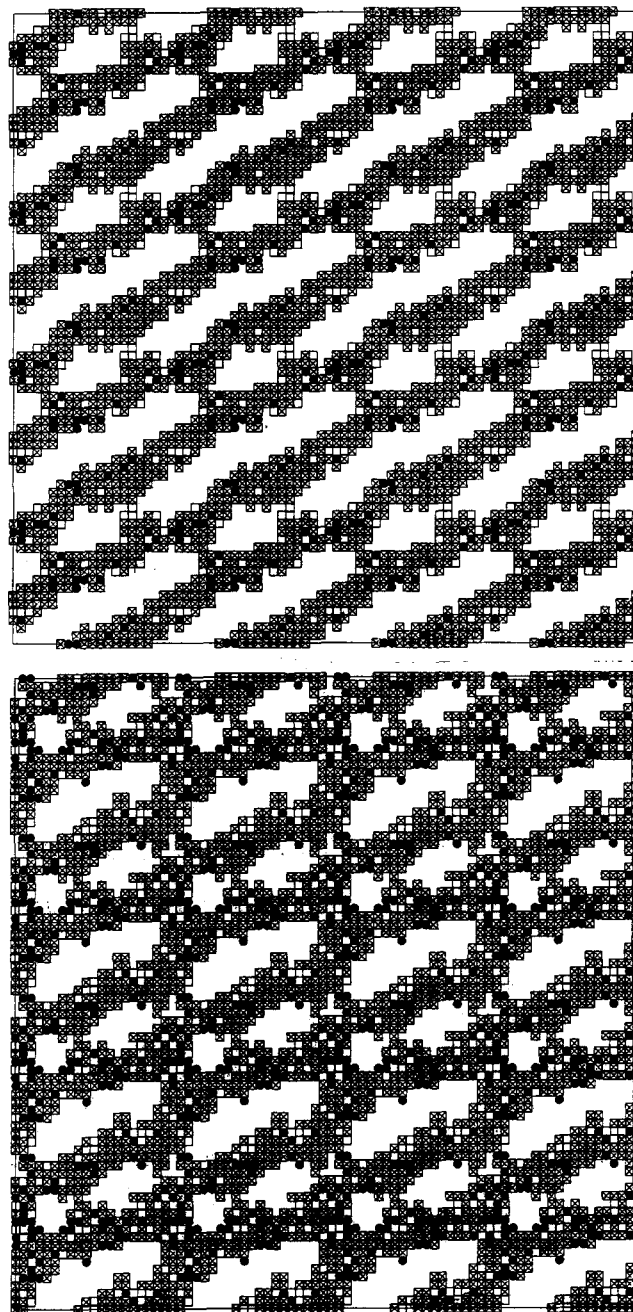


Figure 1. (a, top) One slice in a cubic lattice for a Monte Carlo simulation modeling an AB symmetric, diblock copolymer of 8 total units mixed with an A homopolymer of 8 units in length. Blank spaces are the B segments of the copolymer, \blacksquare represent the A segments of the copolymer, \bullet are the A homopolymer segments, and \square are sites occupied by A solvent molecules. The simulation was for a $20 \times 20 \times 20$ lattice. The 80×80 slice shown here was produced by periodic imaging. (b, bottom) Same as Figure 1a, but showing a different slice in the cubic lattice.

Parts a and b of Figure 3 show slices through the lattice for the case where the homopolymer is 20 sites long; i.e., the homopolymer is 5 times the length of the copolymer blocks. As can be seen in Figure 3a, the system still displays a lamellar morphology. However, the results in Figure 3a,b clearly show that the A homopolymers form aggregates. In fact, the aggregates form bridges between two different A layers of the diblock lamellar morphology. The fact that this structure is not present in Figure 3a indicates that the aggregates are confined or localized within the sample. In the case where the homopolymer is 10 times the length of the blocks (40 sites), the homopolymer aggregation is equally dramatic, as seen in Figure 4b. Another slice in the sample (Figure 4a) is essentially devoid of homopolymer sites, again indicating that this aggre-

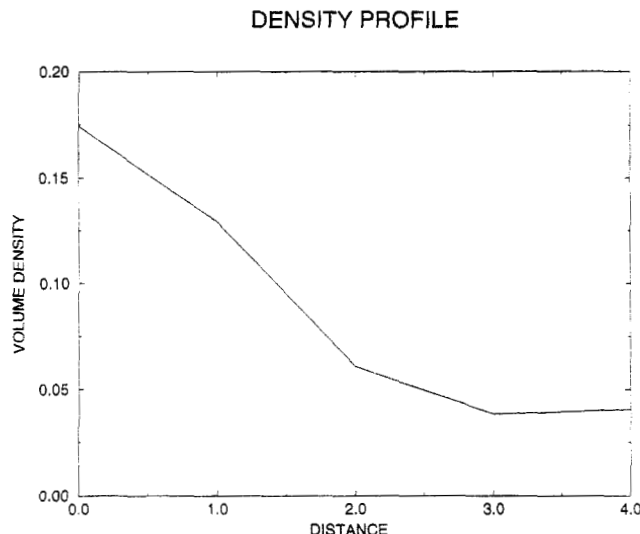


Figure 2. Distribution of homopolymer segments normal to the lamellar surface for the mixture in Figure 1. Zero corresponds to the center of the A lamellae.

gation is highly localized in space.

To quantify this localization, the pair correlation function of the homopolymer units can be calculated by

$$g_H(i) = \frac{3\langle n_H(i) \rangle}{4\pi(i^3 - (i-1)^3)}$$

where $\langle n_H(i) \rangle$ is the average number of homopolymer units located at a distance between $i-1$ and i from a given homopolymer site. Figure 5 shows three $g_H(i)$ curves corresponding to the three different homopolymer lengths. The sharply peaked curves for the chains of lengths 20 and 40 confirm that the homopolymer is localized to a small region within the lattice. It must be noted that $g_H(i)$ is obtained in three dimensions, irrespective of the orientation of the lamellar microdomains, and serves only to characterize the average spatial distribution of the homopolymer segments. The results from both the 20 and 40 site homopolymer simulations clearly show an exclusion of the homopolymer from the lamellar microdomains, a retention of the overall periodic structure, and an incorporation of the aggregates within the periodic structure.

In order to determine if our results were biased by finite size effects, we ran a simulation in a box that is 40×40 lattice sites in size. This was done for the case in which the homopolymers are 40 units long. Parts a and b of Figure 6 show the same characteristics as Figure 4a,b, respectively. (The 80×80 figures now represent periodic images of the 40×40 results.) Thus, we could conclude that these results are not an artifact of lattice size.

There are, however, limitations to the quantitative analyses that we can make with this model. Namely, we cannot accurately measure the width of the lamellar spacing. There are fluctuations in the width of the layer as we go from one plane to another in the box. Averaging over the values for each of the 20 planes yields relatively large error bars. These large error bars mask any differences that arise from increasing the length of the homopolymer. This fact prevents us from making more quantitative comparisons with the experimental system. (Experimental values for the lamellar spacings are given in ref 9.) However, we can nonetheless draw qualitative conclusions from these studies, which we describe below.

When the A homopolymer becomes significantly longer than the A block of the diblock, it is entropically unfavorable for the long chains to be confined in the A layer; however, it is energetically unfavorable for the chains

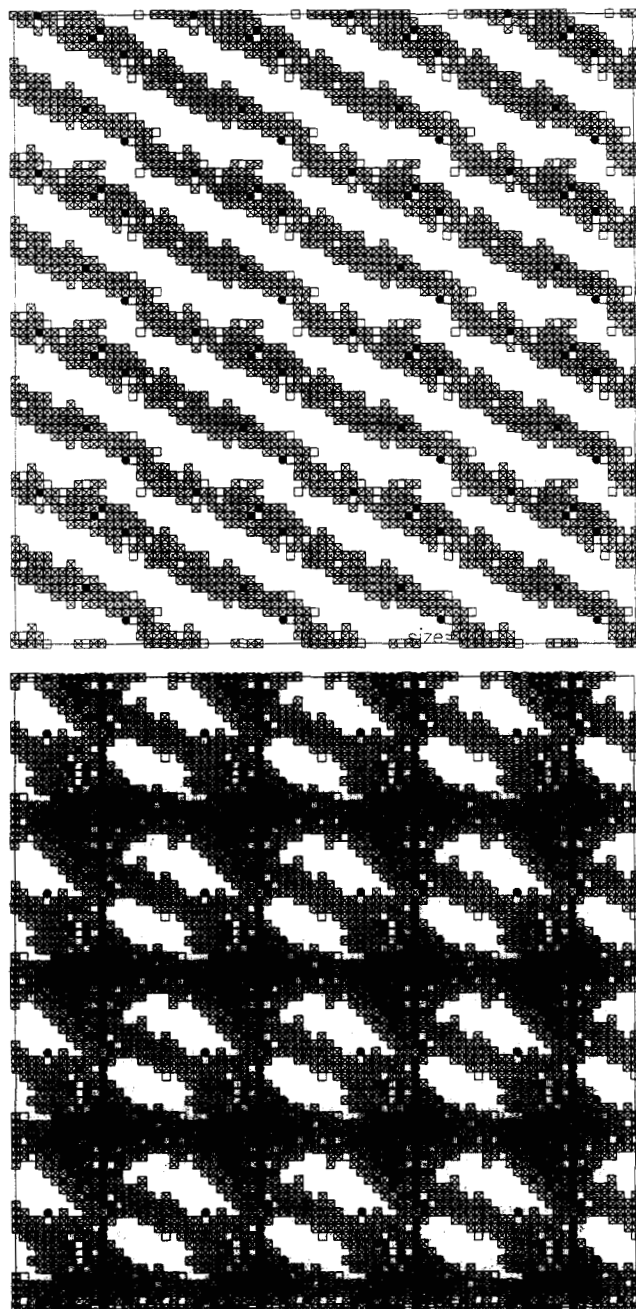


Figure 3. (a, top) One slice from a cubic lattice for a Monte Carlo simulation of a mixture of A homopolymer with 20 lattice sites with an AB diblock copolymer having 8 total lattice sites. The designation of the sites is the same as in Figure 1. (b, bottom) Same as in Figure 3a, but showing a different slice in the cubic lattice.

to extend into the B region. The aggregation of the homopolymers into domains allows the homopolymers to assume a more Gaussian configuration rather than being highly confined and extended within the lamellar microdomains of the copolymer. By aggregating, the chains are also shielded from unfavorable interactions with the B's, in much the same way that aggregated hydrophobic chains are shielded from an aqueous environment. Comparing the results for short and long homopolymers (at a fixed volume fraction of 10%), we can conclude that there is a critical ratio of the homopolymer length to the length of the comparable species in the diblock at which the homopolymers start to undergo this aggregation behavior.

Experiments

Transmission electron microscopy (TEM) measurements were performed on mixtures of a symmetric diblock copolymer of

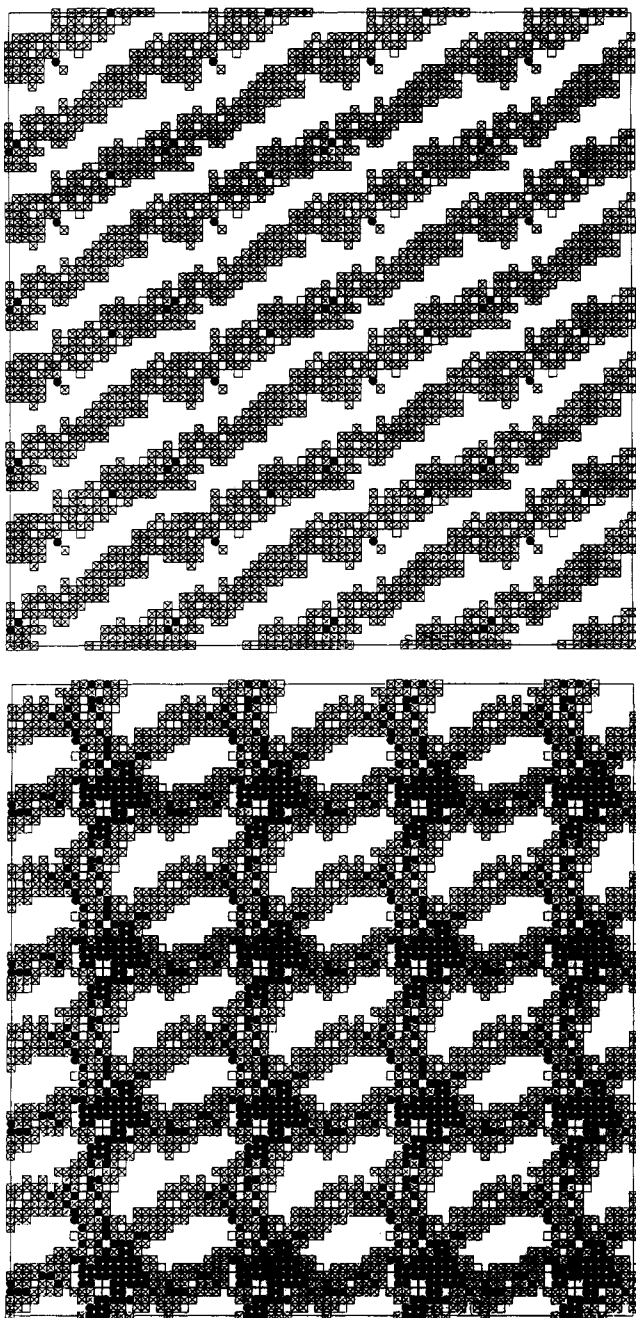


Figure 4. (a, top) One slice of a cubic lattice from a Monte Carlo simulation of a mixture of A homopolymer of 40 sites in length with a symmetric, diblock copolymer of 8 total lattice sites. The site designations are the same as in Figure 1. (b, bottom) Same as in Figure 4a, but showing a different slice in the cubic lattice.

polystyrene, PS, and poly(methyl methacrylate), PMMA, denoted P(S-*b*-MMA), with PS homopolymer. The copolymer molecular weight was $M_w = 9.1 \times 10^4$ ($M_w/M_n = 1.05$), with a PS volume fraction of 0.47. Two different PS homopolymers were used: with $M_w = 5.0 \times 10^4$ ($M_w/M_n = 1.05$) and $M_w = 5.0 \times 10^5$ ($M_w/M_n = 1.06$). Mixtures composed of 10% PS and 90% P(S-*b*-MMA), by weight, were dissolved in toluene and spin coated onto the substrate. The specimen was then annealed at 160 °C for 120 h under vacuum to orient the lamellar microdomains parallel to the film surface. This procedure has been described previously.¹⁶⁻¹⁸

In order to perform the TEM studies, the samples had to be microtomed normal to the surface of the specimen to obtain an edge view of the lamellar multilayer. To this end, the substrates used in this study consisted of a 2-mm-thick sheet of polyimide onto which 500 Å of Au was evaporated. This provided a pure Au surface onto which the copolymer film was placed yet allowed the films to be easily microtomed so that true cross sections of the morphology could be obtained.¹⁹ To enhance the contrast of the lamellar microdomains, the thin cross sections were exposed

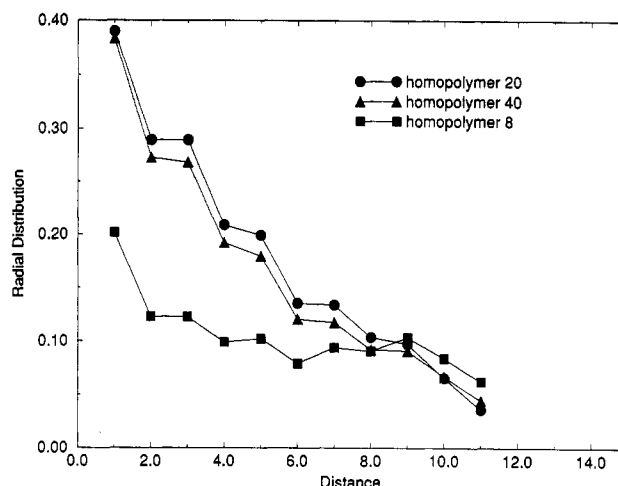


Figure 5. Radial distribution function of homopolymer segments where the total copolymer length is 8 lattice sites and the homopolymer has a length of 8, 20, or 40 lattice sites. Note the localization of the homopolymer as the molecular weight increases.

to RuO₄ vapor for 15 min, which preferentially stained the PS. One note in passing is that studies were performed as a function of exposure time to the RuO₄ vapors. Extended exposure was found to induce artifacts in the morphology. The time of 15 min was determined to be optimal in balancing the enhanced contrast and sample damage. TEM studies were performed on a Zeiss CEM 902 operated at 80 kV.

Discussion of Experimental Results

Figure 7 shows the micrograph of a mixture of 10% PS ($M_w = 5 \times 10^4$) with P(S-*b*-MMA). First, the dark band across the middle of the micrograph is the 500-Å layer of Au. Adjacent to this, a layer of PS is seen, followed by a lighter layer of PMMA. This is then followed by alternating layers of PS and PMMA forming the multilayered morphology. As seen, a PS microdomain is located at the air surface as would be expected from the lower surface energy of PS in comparison to PMMA. Under the conditions of these experiments, the total film thickness is given by nL , where n is an integer and L is the period of the lamellar microdomains. This is in keeping with previous findings.^{16,20}

In Figure 7, the PMMA layers are much thinner than the PS layers, even taking into account the increase of the PS microdomain due to the addition of the PS homopolymer. This results from a degradation of the PMMA in the electron beam, which is followed by a shrinkage of the PMMA domains. In addition, the narrow bridges that span from one PS layer to another have been found to result from the staining procedure and are not characteristic of the multilayered lamellar morphology. Nonetheless, the picture that is evident for thin films of these mixtures is a simple multilayered lamellar morphology where the homopolymer is incorporated within the lamellar microdomains. This should be compared to the results from the simulations shown in Figure 1a,b. As can be seen, the two are in good agreement. It should be noted, though, that the simulations were performed on a system where the molecular weight of the homopolymer was twice that of the copolymer blocks. Consequently, one sees some evidence of weak bridging between the lamellae in Figure 1b.

No information can be obtained from the micrographs on the distribution of the homopolymer within the lamellar microdomains. To do this, a technique like neutron reflectivity must be used where the homopolymer is labeled with deuterium. Independent neutron reflectivity studies were performed on these mixtures on Si substrates, and only the final results will be shown here.⁹ Figure 8 shows

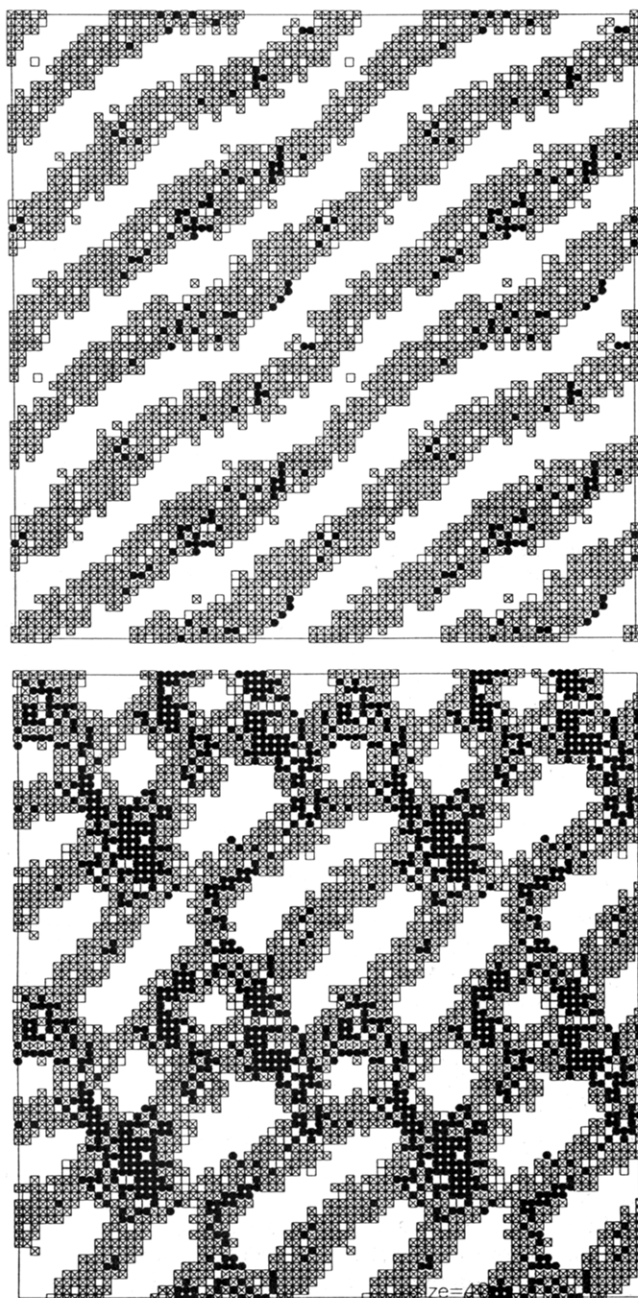


Figure 6. (a, top) One slice of a cubic lattice from a Monte Carlo simulation of a mixture of A homopolymer of 40 sites in length with a symmetric, diblock copolymer of 8 total lattice sites. The box is now $40 \times 40 \times 40$ lattice sites in size. The site designations are the same as in Figure 1. (b, bottom) Same as Figure 6a, but showing a different slice in the cubic lattice.

the distribution of PS homopolymer segments in the multilayered morphology as a function of distance normal to the lamellar surface. Zero has been taken as the center of the PS microdomain, and the vertical dashed lines represent the approximate location of the center of the interfaces between the PS and PMMA layers. One observes that the 5×10^4 molecular weight homopolymer (dashed line) is distributed throughout the microdomain, but the concentration is peaked at the center. While the homopolymer penetrates well into the interfacial region, it is completely confined to this domain, with no homopolymer penetrating deeply into the adjacent PMMA layers. The shape of the distribution agrees well with the simulation results presented in Figure 2.

If the molecular weight is increased to 5×10^5 , however, a completely different morphology is seen. Shown in Figure 9 is a typical micrograph for a system with 10% PS

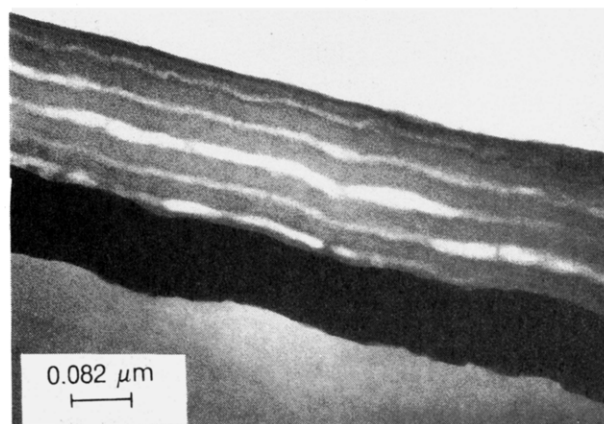


Figure 7. TEM micrograph of a mixture of 10% PS ($M_w = 5 \times 10^4$) with a P(S-*b*-MMA) symmetric diblock copolymer having a total molecular weight of 9.1×10^4 . The sample was spin coated onto a Au-coated polyimide substrate, annealed for 120 h under vacuum at 160°C , and microtomed normal to the film surface. Staining with RuO_4 makes the PS layers appear dark.

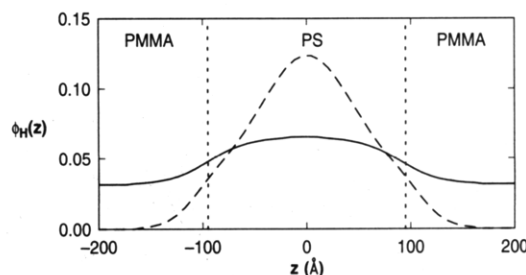


Figure 8. Distribution of PS homopolymer segments as a function of distance normal to the lamellar surface for 10% mixtures of PS homopolymers having $M_w = 5 \times 10^4$ (---) and 5×10^5 (—) with P(S-*b*-MMA) symmetric, diblock copolymer ($M_w = 9.1 \times 10^4$). The vertical dashed lines are the approximate midpoints of the interfaces between the PS and PMMA microdomains.

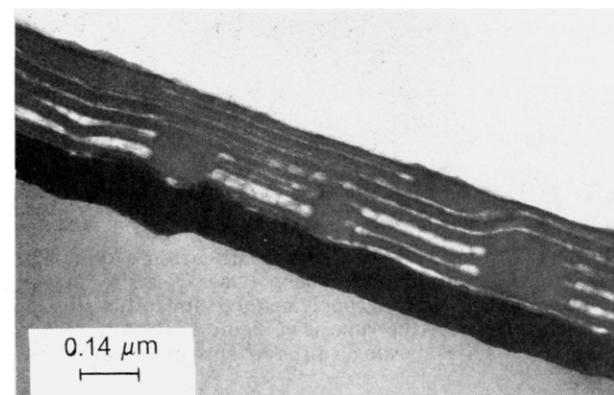


Figure 9. Cross sectional TEM micrograph for a mixture of 10% PS (5×10^5) with a P(S-*b*-MMA) symmetric, diblock copolymer ($M_w = 9.1 \times 10^4$) cast onto a Au-coated polyimide substrate. The sample was annealed for 120 h at 160°C under vacuum, microtomed normal to the surface, and stained with RuO_4 . The dark regions correspond to the PS segments of the homopolymer and copolymer.

($M_w = 5 \times 10^5$) in P(S-*b*-MMA). Immediately obvious in this micrograph are large PS domains scattered throughout the film. While TEM cannot differentiate between the PS segments of the homopolymer or copolymer, it is quite reasonable to conclude that these large domains are formed by the homopolymer that is excluded from the lamellar microdomains. It should be noted that these domains are seen uniformly throughout the film, i.e., at both the air and substrate interfaces, as well as in the interior of the film. Remarkably, the presence of these homopolymer aggregates has not perturbed the multilayered morphology,

but they are incorporated quite nicely into the multilayered structure.

The micrograph in Figure 9 bears a striking resemblance to the results of the simulations shown in Figures 3, 4, and 6. In both the experiment and simulations, the homopolymer is seen to be excluded from the lamellar microdomain morphology.⁹

Again, independent neutron reflectivity measurements on these mixtures, where the PS homopolymer was labeled with deuterium, provided the distribution of the PS homopolymer segments in the multilayered morphology. This is shown in Figure 8 by the solid line. Here, the homopolymer appears to be in both the PS and PMMA layers. This results from the fact that the neutron reflectivity measurements provide a composition profile normal to the surface averaged over the coherence length of the neutrons, which is microns in size. Consequently, the presence of the homopolymer aggregates spanning across the PMMA layers would produce this result. (It is difficult to extract this information from the simulations since density fluctuations at the interface (the interfacial "roughness") are comparable to the layer thickness.)

In conclusion, qualitative agreement between actual experiments and computer simulations has been shown for mixtures of homopolymers with symmetric diblock copolymers. It is clearly shown that, as the molecular weight of the homopolymer is increased above that of the corresponding copolymer blocks, the homopolymer is excluded from the lamellar microdomains, forming aggregates. These aggregates, however, do not markedly perturb the alternating, lamellar microdomain morphology.

The interesting morphologies observed in this study are a product of the competition between the ordering of the copolymer and the macroscopic phase separation of the homopolymer from the copolymer. Since the high molecular weight homopolymer is essentially insoluble in the copolymer, the favored thermodynamic state is a coarsely phase separated system that minimizes the interfacial area between the two. On the other hand, the local organization of the copolymers into lamellar microdomains occurs rapidly in comparison to the long-range diffusion of the homopolymer. Thus, the mixture is trapped in a metastable state that strikes a compromise between these competing processes. What is most intriguing is that the

simulations and the experiments reveal nearly identical frozen-in states.

Acknowledgment. A.C.B. gratefully acknowledges financial support from the Department of Energy, through Grant No. DE-FG02-90ER45438, the National Science Foundation, through Grant No. DMR-9107102, and PPG Industries. The experimentalists are grateful to the Sonderforschungsbereich 60 at the Universität Freiburg for use of their electron microscopy facilities. The experimental work was partially supported by the Department of Energy, Office of Basic Energy Sciences, under Contract DE-FG03-88ER-45375.

References and Notes

- (1) Thomas, E. L.; Alward, D. B.; Kinning, D. J.; Martin, D. C.; Handlin, D. L.; Fetters, L. J. *Macromolecules* **1986**, *19*, 2197.
- (2) Hasegawa, H.; Tanaka, H.; Yamasaki, K.; Hashimoto, T. *Macromolecules* **1987**, *20*, 1651.
- (3) Olvera de la Cruz, M.; Mayes, A. M.; Swift, B. W. *Macromolecules* **1992**, *25*, 944.
- (4) Almadahl, K.; Koppi, K. A.; Bates, F. S. *Macromolecules* **1992**, *25*, 1743.
- (5) Hashimoto, T.; Tanaka, T.; Hasegawa, H. *Macromolecules* **1990**, *23*, 4378.
- (6) Tanaka, H.; Hasegawa, H.; Hashimoto, T. *Macromolecules* **1991**, *24*, 240.
- (7) Tanaka, H.; Hashimoto, T. *Macromolecules* **1991**, *24*, 5712.
- (8) (a) Winey, K. I. Ph.D. Thesis, University of Massachusetts, 1991. (b) Winey, K. I.; Thomas, E. L.; Fetters, L. J. *Macromolecules* **1991**, *24*, 6182.
- (9) Mayers, A. M.; Russell, T. P.; Satija, S. K.; Majkrzak, C. F. *Macromolecules* **1992**, *25*, 6523.
- (10) Shull, K. R.; Winey, K. I. *Macromolecules* **1992**, *25*, 2637.
- (11) Banaszak, M.; Whitmore, M. D. *Macromolecules* **1992**, *25*, 2757.
- (12) Larson, R. G.; Scriven, L. E.; Davis, H. T. *J. Chem. Phys.* **1985**, *83*, 2411.
- (13) Larson, R. G. *J. Chem. Phys.* **1989**, *89*, 1642.
- (14) This value of ω corresponds to a temperature that is approximately 60% of the critical temperature for oil/water mixtures.
- (15) We note that Larson also used a cubic lattice that is 20 sites on a side. The length of his chains was 8 lattice sites, which is also the length of our diblock copolymers.
- (16) Coulon, G.; Russell, T. P.; Deline, V. R.; Green, P. F. *Macromolecules* **1989**, *22*, 2581.
- (17) Russell, T. P.; Coulon, G.; Deline, V. R.; Miller, D. C. *Macromolecules* **1989**, *22*, 4600.
- (18) Anastasiadis, S. H.; Russell, T. P.; Satija, S. K.; Majkrzak, C. F. *J. Chem. Phys.* **1990**, *92*, 5677.
- (19) Kunz, M.; Shull, K. R. *Polym. Commun.*, submitted for publication.
- (20) Foster, M. D.; Sikka, M.; Singh, N.; Baks, I. S.; Satija, S. K.; Majkrzak, C. F. *J. Chem. Phys.*, in press.